

1 **A RETINOBLASTOMA-RELATED transcription factor network governs egg cell**  
2 **differentiation and stress response in *Arabidopsis***

3

4 **A transcription factor network impinges on eggs (short title)**

5

6 Olga Kirioukhova-Johnston<sup>1,2</sup>, Pallavi Pawar<sup>1¶</sup>, Geetha Govind<sup>1¶a</sup>, Pramod Pantha<sup>3</sup>,

7 René Lemcke<sup>1,4b</sup>, Vidhyadhar Nandana<sup>1c</sup>, Danaé S. Larsen<sup>1</sup>, Alagarsamy M.

8 Rhahul<sup>1</sup>, Jubin N. Shah<sup>1</sup>, Patrick von Born<sup>1d</sup>, Chathura Wijesinghege<sup>3</sup>, Yue Zhou<sup>5d</sup>,

9 Wilhelm Gruissem<sup>6</sup>, Franziska Turck<sup>5</sup>, Maheshi Dassanayake<sup>3\*</sup>, Amal J.

10 Johnston<sup>1,2,4\*</sup>

11

12 <sup>1</sup>Centre for Organismal Studies (COS), University of Heidelberg, Heidelberg,

13 Germany

14 <sup>2</sup>Institute of Biology, Freie Universitaet Berlin, Berlin, Germany

15 <sup>3</sup>Department of Biological Sciences, Louisiana State University, Baton Rouge, USA

16 <sup>4</sup>Leibniz Institute of Plant Genetics and Crop Plant Research, Gatersleben, Germany

17 <sup>5</sup>Max-Planck-Institute for Plant Breeding Research, Cologne, Germany

18 <sup>6</sup>Department of Biology and Zurich-Basel Plant Science Center, ETH Zurich, Zurich,

19 Switzerland

20

21 <sup>a</sup>Present address: Department of crop physiology, College of Agriculture, University

22 of Agricultural Sciences, Hassan, India

23 <sup>b</sup>Present address: Department of Plant and Environmental Sciences, University of

24 Copenhagen, Frederiksberg, Denmark

25 <sup>c</sup>Present address: Division of Biochemistry, Freie Universitaet Berlin, Berlin,  
26 Germany

27 <sup>d</sup>Present address: Centre for Life Sciences, Peking University, Beijing, China

28

29 \*Corresponding authors:

30 [amal.johnston@greentechlab.net](mailto:amal.johnston@greentechlab.net)

31 [maheshid@lsu.edu](mailto:maheshid@lsu.edu)

32

33 <sup>¶</sup>These authors contributed equally to this work

34 **Abstract**

35

36 The multicellular embryo, and ultimately the entire organism, is a derivative of the fertilized  
37 egg cell. Unlike in animals, transcription factor networks orchestrating faithful egg  
38 development are still largely unknown in plants. We have identified that egg cell  
39 differentiation in *Arabidopsis* require interplay between evolutionarily conserved onco-protein  
40 homologs RETINOBLASTOMA-RELATED (RBR) and redundant MYB proteins  
41 MYB64/MYB119. RBR physically interacts with the MYBs; and with plant-specific  
42 transcription factors belonging to the RWP-RK-domain (RKD) family and LEAFY  
43 COTYLEDON1 (LEC1), which participate in development of egg cells and inherent stress  
44 response. RBR binds to most of these egg cell-expressed loci at the DNA level, partially  
45 overlapping with sites of histone methylation H3K27me3. Since deregulation of *RKDs*  
46 phenocopies mutants of *RBR* and the *MYBs* in terms of cell proliferation in the egg cell  
47 spatial domain, all the corresponding proteins are likely required to restrict parthenogenetic  
48 cell divisions of the egg cells. Cross-talk among these transcription factors, and direct  
49 regulation by RBR, govern egg cell development and expression of egg-to-zygotic polarity  
50 factors of the WUSCHEL RELATED HOMEODOMAIN family. Together, a network of RBR-  
51 centric transcription factors underlies egg cell development and stress response, possibly, in  
52 combination with several other predicted nodes.

53

54

55

56 **Key words**

57 egg cell | transcription factor | RETINOBLASTOMA RELATED | MYB | RKD | stress |  
58 parthenogenesis

59

60 **Author summary**

61

62 The RETINOBLASTOMA protein is one of the core components of the Eukaryotic  
63 cell cycle, and corresponding evolutionary homologs have been implicated not only  
64 to repress cell division but also to control differentiation and development. How  
65 RETINOBLASTOMA RELATED (RBR) associate with other higher order regulators  
66 to control faithful egg cell development in sexual plants is pivotal for manipulation of  
67 successful reproduction in general, and engineering of parthenogenesis when  
68 asexual or apomictic seed progeny are desirable over sexual plants. Using a suite of  
69 molecular methods, we show that a RBR-associated transcription factor network  
70 operates to specify egg cells in *Arabidopsis*. Complex cross-regulation within these  
71 transcription factors seems to be necessary for successful maternal egg cell to  
72 zygotic transition and reproductive stress response. Detailed genetic analysis  
73 implicate that RBR and its interactive partners belonging to MYB and RWP-RK  
74 transcription factor families are possibly required to prevent parthenogenesis of the  
75 sexual egg cells. Novel RBR networks and stress nodes explained in this study  
76 might help to improve our understanding of sexual and asexual reproduction.

77

78

79

## 80 **Introduction**

81 Proper differentiation of the egg cells is pivotal for sexual reproduction as well as  
82 parthenogenesis. In flowering plants, the egg cells are terminally differentiated within  
83 the miniature female gametophyte structures known as the embryo sacs that are  
84 encased by layers of sporophytic cells in the ovule. Cellular differentiation and  
85 maintained homeostasis are crucial for egg cell development, and they have been  
86 proposed to be orchestrated by positional cues during establishment of ovule and  
87 embryo sac polarity [1-6], and ultimately of the egg cell and zygote [7,8] in  
88 *Arabidopsis*. Tightly coordinated developmental processes implicate both directed  
89 cell-to-cell communication and cell-autonomous regulation operating throughout  
90 embryo sac development and fertilization processes.

91 Egg cell development in plants is proposed to be under the control of molecular  
92 factors including cell cycle regulators, transcription factors, RNA splicing machinery,  
93 signalling molecules such as secreted peptides and chromatin dynamics {reviewed  
94 in [1]}. Transcription factors play a predominant role in regulation of gene expression,  
95 thus, tight control over transcriptional regulation is foreseeable in the egg cell [9,10].  
96 A microarray expression analysis of the *Arabidopsis* egg cell transcriptome suggests  
97 that >350 transcription factors could be expressed there [9]. Although this is likely an  
98 underestimate, considering the difficulty in isolating the *Arabidopsis* egg cell over  
99 that of rice [10], large transcription factor families such as MYB, RWP-RK domain-  
100 containing (RKD) and WUSCHEL-RELATED HOMEODOMAIN (WOX) have been  
101 proposed to be prominent members of the egg cell transcriptome [1,9]. Functional  
102 dissection of these egg cell-expressed transcription factors, and exploring the

103 inherent cross-talks and associated networks, will give a clear picture of egg cell  
104 determination and patterning in plants.

105 A unique feature of the egg cell in sexually reproducing organisms is a temporary  
106 arrest of its cell divisions until fertilization and reprogramming to zygotic gene  
107 expression. In flowering plants, deregulation of a homologue of *BABYBOOM* (*BBM*)  
108 [11], *MULTI-SUPPRESSOR OF IRA 1* (*MSI1*) [12] and specific R2R3-type *MYBs*  
109 [13] are implicated in autonomous developmental events in the embryo sac and in  
110 particular the egg cell. In *Arabidopsis*, overexpression of *WUSCHEL*, *MYB* genes,  
111 *BBM*, and *LEAFY COTYLEDON1* (*LEC1*) has been shown to induce somatic  
112 embryogenesis [14-16], indicating that they participate in transcriptional rewiring  
113 towards embryo development. *LEC1* encodes a CCAAT-box binding transcription  
114 factor known primarily for its role during embryogenesis, seed maturation and stress  
115 amelioration [17,18]. Interplay of *WUSCHEL*-related transcription factors *WOX2* and  
116 *WOX8* prepares the egg cell to establish zygote polarity [8]. Unlike the neighbouring  
117 central cell, the egg cell chromatin environment is rather transcriptionally quiescent  
118 with high levels of repressive histone methylation marks such as H3K27me3 [19,20].  
119 Nevertheless, combinatorial transcription factor regulation and epigenetic  
120 modifications likely play an important role during egg cell development in plants.

121 Ready for fertilization, the egg cell in *Arabidopsis* likely stays quiescent in the G2-  
122 phase of the cell cycle, thus matching the cell cycle stage of the sperm cell at the  
123 onset of fertilization [21]. Only a few cell cycle regulators are expressed in the egg  
124 cell [9], including the higher-order transcriptional repressor *RETINOBLASTOMA*  
125 *RELATED* (*RBR*). Deregulation of *RBR* has been shown to perturb egg cell  
126 specification and genome integrity [22-24]. While *RBR* and its paralogues control

127 transcriptional networks in somatic cell types, either dependent or independent of the  
128 cell cycle [25,26], whether they play a similar role in egg cell development is  
129 currently not understood. In this study, we have established functional links between  
130 RBR and a subset of transcription factors controlling egg cell development and  
131 stress response during *Arabidopsis* reproduction. Notably, we have demonstrated  
132 the importance of an RBR-centric egg cell-expressed transcription factor network  
133 essential for sexual and parthenogenetic reproduction, and have identified several  
134 putative nodes of this network for further dissection.

135

## 136 **Results**

### 137 ***RBR* is required for egg cell development**

138 In order to understand the true expression of RBR during egg cell development, we  
139 constructed a reporter line consisting of an N-terminal fusion of GFP to a genomic  
140 *RBR* locus that was driven under its 2.2 Kbp promoter and included 3' flanking  
141 region (*pRBR::GFP-RBR*). To test the functionality of the construct, first we  
142 introduced the transgene into the amorphic *rbr-3 Arabidopsis* mutant in which the  
143 entire embryo sac is defective and cells proliferate instead of appropriate cell  
144 differentiation [6,24]. Screening multiple independent transformants, we recovered  
145 *pRBR::GFP-RBR* lines that were able to completely restore the wild-type function of  
146 *RBR* in the female gametophytes. These transgenics fully rescued the *rbr-3*-  
147 mediated ovule sterility, as evident from restored seed set, and transmission of the  
148 mutant allele to the progeny (Fig 1A-B, Table S1-S2). Therefore, the *pRBR::GFP*-  
149 *RBR* was sufficient for development of the embryo sac including the egg cell. Next,  
150 we examined these transgenics for expression of GFP, which would correspond to

151 the endogenous localization of RBR. Consistent with the phenotypic  
152 complementation, we detected the recombinant protein produced by the  
153 *pRBR::GFP-RBR* construct in the synergids and the egg cell (Fig 1C). Upon egg cell  
154 fertilization, the *pRBR::GFP-RBR* signal decreased in the zygote to almost  
155 undetectable level (Fig 1C-E). Thus the egg apparatus expression of RBR under its  
156 native promoter was sufficient for proper egg differentiation, and a rapid reduction of  
157 RBR upon fertilization must have been important for egg-to-zygote transition.

158 To test whether RBR expression in the egg cell alone is sufficient to restore its wild-  
159 type function, we expressed a *tagRFP-RBR* fusion under a strong egg cell-specific  
160 promoter of *EGG CELL 1.1* (*pEC*) [27] (*pEC::tagRFP-RBR*) (Fig. 1F) and introduced  
161 it into the *rbr-3* mutant too. Indeed, *pEC::tagRFP-RBR* construct could partially  
162 rescue the null *RBR* mutation as evident from improved seed set and strong  
163 increase of *rbr-3* allele transmission to the progeny from 7% in *rbr-3/+* alone [22] to  
164 25% in the presence of the transgene (Fig.1A-B; Table S3-S4). Notably, the strong  
165 overexpression of *RBR* in the egg cell, as visualized by expression of tagRFP, did  
166 not cause obvious aberrations in the embryo sac nor seed development in the wild-  
167 type background. Taken together, data as above suggest that the amount of RBR  
168 under its native promoter is sufficient for egg cell development, while its increased  
169 dosage in the egg cell does not perturb sexual reproduction.

## 170 **RBR-dependent transcriptional regulation in the egg cell**

171 Since abolishing RBR expression caused severe perturbations in egg cell  
172 differentiation, development and function [22], and that these developmental  
173 anomalies could be restored when RBR is expressed specifically in egg cell (Fig. 1A-  
174 B,F), we reasoned that most of the phenotypic effects observed in the *rbr-3* mutant



175 were due the absence of RBR expression in the egg cell. Therefore, we made use of  
176 the amorphic *rbr-3* mutant to uncover the transcriptional changes in the egg cell  
177 upon depletion of *RBR* by comparing transcriptional profiles of the mutant ovules  
178 against the wild-type ovules. We assumed that differences between transcriptomes  
179 of *rbr-3* and wild-type ovules should reflect mainly the female gametophyte-specific  
180 gene expression [2,6,28], for *RBR* gene is haplosufficient both in sporophytic and  
181 gametophytic tissues [22]. We conducted a two-step comparative transcriptome  
182 analysis. In step-1, all the acquired mRNA-seq data from the ovules were filtered to  
183 retain those genes reported as part of the *Arabidopsis* egg cell microarray dataset  
184 [9]. In step-2, the filtered data were subjected for wild-type versus mutant differential  
185 expression analysis. This approach allowed us to scrutinize egg cell-related gene  
186 expression profiles of the wild-type versus *rbr-3* genotypes.

187 Differential gene expression analysis identified a total of 2096 egg cell-expressed  
188 genes with over 20 transcripts that were previously validated for spatial egg cell  
189 expression (Table S5, Fig. 2A-B). GO enrichment analysis of the egg cell-expressed  
190 transcripts pinpointed several transcription factors (105) and stress-related genes  
191 (172) that potentially could function downstream of *RBR* (Table S6, Fig. S1). Among  
192 *rbr-3* up- and down-regulated genes, 120 and 70 candidates, respectively, (ca. 9%)  
193 fell under GO categories related to stress. Interestingly, 18% of transcription factors  
194 upregulated in *rbr-3* were stress-related versus 7% that were down-regulated,  
195 indicating a predominant repressive function of RBR on transcriptional regulators  
196 involved in stress responses in the egg cell.

197 In order to validate the mRNA-seq data and to build up a functional egg cell-  
198 associated transcriptional regulatory network, we chose specific differentially

199 expressed candidate genes that have been known for their egg cell expression [9] or  
200 function. We confirmed downregulation of egg cell-expressed genes *EGG CELL 1.1*  
201 (*EC1.1*) [27] and *WOX8*, and upregulation of *WOX2* [8,29] and *ETHYLENE*  
202 *RESPONSE FACTOR 104 (ERF104)* [9] by qRT-PCR (Fig. 2C-F). In addition,  
203 abundant *EC1.1* mRNA *in situ* signals were readily visible in the wild-type egg cell;  
204 however, in *rbr-3* eggs, *EC1.1* signals were partially depleted (Fig. 2D-E). Validating  
205 the spatio-temporal gene expression profile of egg-cell specific markers such as  
206 *EC1.1* served as a quality control of our genetic subtraction approach.

207 While the egg-like cells of *rbr-2* embryo sacs still expressed promoter reporters of  
208 female gametophyte-expressed MYB transcription factors *pMYB64::GFP* and  
209 *pMYB119::GFP* [13], our mRNA-seq analysis on *rbr-3* ovules identified *MYB64* as a  
210 differentially expressed transcript (Table S5). Indeed, validation by real-time qRT-  
211 PCR confirmed a slight but statistically significant upregulation of *MYB64* in *rbr-3*  
212 ovules (Fig. 2G). *MYB64* was found to be functionally redundant with *MYB119*, and  
213 double *myb64;myb119* mutants showed severe aberrations in embryo sac  
214 development including egg-cell like proliferation almost phenocopying amorphic *rbr*  
215 mutations [6,22] (Fig. 1G-H). It is interesting to note that loss of *MYB64;MYB119*  
216 function had a similar effect on *WOX2* and *WOX8* expression (Fig. 2F). Several  
217 double allelic combinations of *myb64* and *myb119* showing similar embryo sac  
218 proliferation phenotypes were elaborated, and were fully rescued in presence of  
219 intact *MYB64* or *MYB119* [13]. We detected mRNA for both genes throughout the  
220 mature embryo sac (Fig. S2), confirming that the previously analysed promoter::GFP  
221 fusions [13] reflected endogenous expression patterns of the corresponding loci.  
222 Further, we noticed that, unlike pRBR::GFP-RBR, pMYB64::MYB64-GFP protein  
223 was rather abundant in the unfertilized egg and in the early zygote (Fig. 1I-K).

224 The transcriptional profile of most of the *RKD* genes pinpointed their preferential  
225 expression in the *Arabidopsis* egg cell [9,30]; however no reports are available on  
226 the corresponding proteins. We found that a *RKD2* protein fusion with GUS ( $\beta$ -  
227 glucuronidase) was localised to the egg cell in *Arabidopsis* (Fig. 1I). *RKD2* was  
228 significantly downregulated at least in *rbr-3* (Fig. 2G). Although *RKD1* gene  
229 expression was slightly down-regulated in *rbr-3* ovules, it was upregulated in  
230 *myb64;myb119* mutant. In contrast, *RKD3* was upregulated in both mutants (Fig.  
231 2G). We found that *LEC1*, a stress-related gene primarily expressed during seed  
232 development, is also expressed in the egg cell. Expression of *pLEC1::GUS* construct  
233 was undetectable in the sporophytic cells of the ovule; however, a faint GUS signal  
234 was recorded throughout the embryo sac including the egg cell (Fig. 1L). Similar to  
235 *RKD3*, *LEC1* transcripts were strongly upregulated in *rbr-3* and *myb64;myb119*  
236 ovules (Fig. 2G). Since *RKD2*, *RKD3* and *LEC1* are commonly deregulated in both  
237 *rbr-3* and *myb64;119* mutant ovules that phenocopy each other, it is apparent that  
238 RBR and MYB64/119 act in the same regulatory pathway upstream of RKDs and  
239 *LEC1* transcription factors during egg cell development.

#### 240 **RBR is tethered to promoters of a subset of egg cell transcription factors**

241 To establish whether the egg cell genes upregulated in the *rbr-3* mutant could be  
242 direct targets of RBR, we performed chromatin immunoprecipitation (ChIP)  
243 experiments. We tested enrichment of promoter fragments of *MYB64*, *LEC1*, *RKD3*  
244 and *WOX2* after immunoprecipitation of GFP-RBR in reproductive tissues that  
245 contained mature egg cells (Fig. 3A-B). A fragment spanning an E2F binding site in  
246 promoter of *PROLIFERATING CELL NUCLEAR ANTIGEN (PCNA)* served as a  
247 positive control for RBR binding, and promoter of *At1g69770* as a negative control

248 [31]. Upon antibody background subtraction, most of the tested fragments were  
249 found RBR-associated (Fig. 3B-C). *pRKD3*, *pWOX2* and *pLEC1* fragments were  
250 enriched in both RBR-ChIPs across vegetative and reproductive stages (Fig. S3A).  
251 The *MYB64* promoter, however, showed differential RBR occupation level at two  
252 tested E2F binding sites between the tissue types. Surprisingly, the *MYB64* gene  
253 body was also bound by RBR. In order to verify RBR targeting both *MYB64* and  
254 *RKD3* directly in the egg cell, we performed an additional ChIP experiment using  
255 *pEC::tagRFP-RBR* transgenics. Here, we examined specific sites of *pMYB64*  
256 (containing predicted canonical E2F sites) and *pRKD3* (no E2F sites) promoters that  
257 we tested earlier for binding by GFP-RBR, upon immuno-precipitation of tagRFP-  
258 RBR. Both *pMYB64* and *pRKD3* promoter fragments were found enriched for this  
259 epitope binding (Fig. 3C), leading us to conclude that RBR represses transcription of  
260 *MYB64* and *RKD3* in the egg cell by directly binding to their corresponding  
261 promoters.

262 Next, we asked if the sites of RBR binding within our target egg cell candidate loci  
263 overlapped with the repressive histone methylation mark H3K27me3, similar to  
264 previous findings in seedling tissues [31]. We performed ChIP for H3K27me3-bound  
265 DNA in egg cell-containing gynoecia using a ChIP experiment on seedlings as a  
266 baseline for chromatin occupation by H3K27me3 (Fig. S3B). A previously reported  
267 fragment with an E2F binding site in the *PCNA* promoter was used as a negative  
268 control for H3K27me3 enrichment [31]. H3K27me3 mark loading in gynoecia tissues  
269 resembled overall that of the seedlings, with significantly lower and higher  
270 enrichment in *RKD3* and *WOX2* promoters, respectively. In both the seedlings and  
271 reproductive tissues, *MYB64* showed low H3K27me3 binding in its promoter similar  
272 to *pPCNA*, and high binding at the coding regions. The *LEC1* locus was moderately

273 decorated with H3K27me3 mark. Our data pinpointed that both RBR and the  
274 Polycomb Repressive Complex 2 (PRC2) with its inherent H3K27me3 activity could  
275 bind to the promoters of the egg cell-expressed transcription factors investigated.

276 **Deregulation of RETINOBLASTOMA network partly phenocopies stress-**  
277 **induced effects on egg cell development**

278 Both *rbr-3* and *myb64;myb119* female gametophytes mostly fail to arrest mitotic  
279 divisions, often showing multiple cells at the position of the egg cell and other cell  
280 types (Fig. 1G-H, 2A, 4A-C). In *Arabidopsis*, there are five *RKD* genes, but their  
281 function during egg cell development is masked due to redundancy and lack of  
282 faithful mutant alleles [30,32]. We previously reported that three *RKD* genes are  
283 preferentially expressed in the egg cell, and act as activators of a subset of unknown  
284 genes expressed there [30] (Fig. 1L). Two other RKDs are also expressed in the egg  
285 cells and also elsewhere in the sporophyte [9,33]. Therefore, we analysed the role of  
286 the *RKD* family by attaching a transcriptionally repressive EAR-domain [34] to *RKD2*  
287 driven by the egg cell-specific *pEC* promoter (referred to as *pEC::RKD<sup>DN</sup>*). Stable  
288 expression of the *pEC::RKD<sup>DN</sup>* transgene in plants led to variable seed set ranging  
289 from 50-75% of viable seeds, and the remaining ovules aborted at early stages. A  
290 number of mutant embryo sacs had additional egg-like cells in the egg apparatus  
291 (N=14/123) (Fig. 4D-E), and some embryo sacs completely collapsed (Fig. 4F). Most  
292 strikingly, when fertilization was blocked, we observed rare cases (N=5/81) of  
293 parthenogenetic zygote/embryo development that subsequently aborted as the  
294 unfertilized central cell failed to produce the endosperm (Fig. 4H-I, compare to  
295 sexual zygote in 4G). Taken together, deregulation of the *RKD* factors partially  
296 resembled loss of RBR or MYB64;MYB119 activity in terms of additional egg cells

297 within the same embryo sac, supporting that they are down-stream and/or a part of  
298 the RBR and MYB pathway operating in the egg cell specification.

299 Several stress genes were deregulated in *rbr-3* grown in ambient conditions (Fig. 2A-  
300 B, 4V, S1), suggesting activation of a cellular stress response in the absence of RBR  
301 function in the embryo sac. We noted that egg cell-expressed stress-response genes  
302 such as *ARABIDOPSIS ZINC FINGER 2 (AZF2)*, *NAC19*, and *BETA-AMYLASE 1*  
303 (*BAM1*) were upregulated not only in *rbr-3* but also in *myb64;myb119* ovules (Fig.  
304 4V). We tested our hypothesis of stress influencing embryo sac or egg cell  
305 development by exposing soil-grown plants to external abiotic stress conditions such  
306 as NaCl, drought, and elevated temperature (27°C). Under salinity stress, we  
307 observed desynchronization of embryo sac development ranging from two-nucleate  
308 to mature four-celled stages in the same flower, while in control 95% of ovules  
309 contained mature embryo sacs (n=157 and 174), indicative of delayed egg cell  
310 development under salt stress. Furthermore, we observed formation of twin egg  
311 cells, and also collapsed embryo sacs under salinity (Fig. 4J-M), while mild drought  
312 led to rather wild-type like ovules with rare observations of additional egg-like cell  
313 along with the fertilized zygote (Fig. 4N-O).

314 The *LEC1* reporter was upregulated in the egg cells upon different stress conditions  
315 (Fig. 4P-S,V), substantiating the anticipated role of *LEC1* in mediating stress  
316 response in the egg cell similarly to other plant organs [reviewed in [35]].

317 Additionally, very strong activation of *LEC1* gene was observed in the egg apparatus  
318 specifically in synergids upon pollen tube entry, suggesting a strong stress response  
319 during programmed cell death of synergid cells (Fig. 4T-U). *RKD* expression  
320 responded to stress in a distinct manner. Both *RKD1* and *RKD3* were mainly

321 upregulated and *RKD2* was downregulated upon stress, suggesting differential  
322 regulation across these redundant and recently-duplicated factors. *MYB64* and  
323 *MYB119* expression was not significantly altered across most stress conditions,  
324 except for downregulation of *MYB64* under elevated temperature. Whether it is (a)  
325 abiotic stress or (b) mutational effects in *rbr-3* and *myb64;myb119* grown under  
326 ambient conditions, it is noteworthy that phenotypic effects like induction of super-  
327 numerary egg cells and transcriptional responses for RBR-regulated genes, are  
328 similar across experiments.

### 329 **Expanding the RBR-centric egg cell network**

330 In addition to the transcriptional regulation centred on RBR and the egg cells in  
331 *Arabidopsis*, we asked if other regulatory cues such as protein-protein interaction  
332 can also be identified for the egg cell-expressed proteins. First, we performed a  
333 heterologous two-hybrid protein-protein interaction experiment in yeast, using RBR  
334 as bait and the egg cell-expressed transcription factors as prey. We used an RBR-  
335 interacting protein MULTI-SUPPRESSOR-OF-IRA 1 (MSI1) as a prey in control  
336 experiments [28]. When RBR was used in binary combinations with MSI1, MYB64,  
337 MYB119, RKD1, RKD2, RKD3 and LEC1, we observed growth of yeast cells in  
338 appropriate drop-out media, hinting that interaction between RBR and these  
339 transcription factors occurred heterologously in yeast (Fig. S4). We validated these  
340 interactions *in vivo* in plant cells by using Bi-molecular Fluorescence  
341 Complementation (BiFC). The transient BiFC in tobacco leaves confirmed that RBR  
342 interacted with MYB64 and MYB119, RKD1-3 and LEC1, although the signals were  
343 rather weak in case of MYB119 and LEC1 (Fig. 5A-B). Concisely, we identified three

344 different groups of transcription factors as part of the RBR egg cell regulatory  
345 network, among which two represent redundant gene families.

346 Whereas the above work established a subset of RBR interactors expressed in the  
347 egg cell, we wanted to supplement this work by building up a putative interaction  
348 map of the RBR egg cell network. We combined the available protein interaction  
349 datasets (Table S7), including those we identified in this work (Fig. 5, S4), and also  
350 we incorporated a subset of putative RBR interactors identified via a large-scale  
351 yeast-two-hybrid study that used a seedlings-specific *Arabidopsis* cDNA library as a  
352 bait (Gruissem lab, unpublished work in collaboration with Hybrigenics SA, Paris,  
353 France). We assumed each putative protein interactor to be present in the egg cell if  
354 the corresponding transcripts were previously identified to be a part of the  
355 *Arabidopsis* egg cell transcriptome [9]. The predicted network as depicted in Fig. S6  
356 pinpointed that the putative RBR-centric egg cell interactome comprised of not only  
357 core cell cycle factors but also several differentiation and abiotic-stress associated  
358 nuclear factors.

359

## 360 **Discussion**

### 361 **RBR & MYBs: cell cycle versus cell-cycle-independent mode of action?**

362 Protein Retinoblastoma (pRB) and many MYB transcription factors are known cell-  
363 cycle regulators and onco-proteins in animal systems, and are part of evolutionarily  
364 ancient protein complexes [36-41]. Whereas pRB/RBR exists as a single or low copy  
365 number genes encoding conserved pocket proteins in animals and plants, the *MYB*  
366 genes that encode typical MYB domain proteins occur as single to multiple copies in



367 animals. However, the plant MYB proteins comprise three subfamilies with some  
368 hundreds of proteins [42]. The MYBs reported here belong to a R2R3-type  
369 subfamily, which contains an additional homeo-domain. Protein interaction between  
370 RBR and MYB64/119 identified here suggests that RBR might form complexes with  
371 the plant MYBs. RBR-MYB protein interactions were previously reported for the cell  
372 cycle-related MYB3R-type proteins in *Arabidopsis* leaves [40] and for metazoan b-  
373 MYBs [43,44]. Deregulation of both *RBR* and *MYB64/119* in *Arabidopsis* leads to  
374 super-numerary cells in the female gametophytes that are partially defective in  
375 establishing respective cell identities, which is reminiscent of cancer-like cell  
376 proliferation and oxidative cellular stress response. Female germline-specific  
377 requirement of RBR and MYBs in *Arabidopsis* and corresponding roles of their  
378 paralogues in mice oocytes [38,45] illustrate how these dual modules might have  
379 retained their common reproductive function in evolution.

380 Three common aspects of the cell cycle regulation involving both RBR and MYB64 in  
381 *Arabidopsis* can be revisited. Firstly, the canonical cell cycle role of RB/RBR is to  
382 repress the transcription of E2F-regulated S-phase genes. Our ChIP data suggest  
383 that RBR might directly repress *MYB64* via an E2F canonical binding site in its  
384 promoter. Though *MYB64* has not been reported as a core cell cycle gene, *MYB64*  
385 transcripts were upregulated during the S-phase in an *Arabidopsis* suspension cell  
386 culture synchronized for cell cycle progression (Fig. S5) [46]. Therefore, we propose  
387 that *MYB64* might indeed be cell cycle regulated in the S-phase in *Arabidopsis*. The  
388 mechanism of MYB transcriptional regulation by RB appears to be evolutionarily  
389 ancient, as exemplified by similar cell-cycle regulation of the human Mybs [47,48].  
390 Secondly, depletion of RBR or MYB64/119 has strikingly similar effects and causes  
391 both rather cell-cycle-independent mis-establishment of cell identities and cell-cycle-

392 dependent proliferation in the embryo sac, particularly of the egg cell [13,22]. Thus, it  
393 is possible that both RBR and MYBs are essential for maintenance of the G2-phase  
394 pre-fertilization arrest and prevention of autonomous mitotic divisions of the egg  
395 cells. However, the mild upregulation of *MYB64* in *rbr-3* was unable to rescue egg  
396 cell function, indicating that complex interplay of both these proteins is necessary  
397 during female gamete development. A third aspect regarding an additional cell cycle  
398 role RBR and MYB64 concerns the mitotic phase. In the mature egg cells, RBR  
399 protein is quite low and MYB64 is rather abundant (Fig, 1C,I). Upon fertilization,  
400 zygotic expression of RBR declines even further, while the MYB64 signal is  
401 maintained at a similar level (Fig. 1C-E,I-K). The low abundance of RBR perhaps  
402 reflects an additional requirement of RBR in regulating mitotic division, similar to the  
403 M-phase-specific role of its paralog *rbIA* in *Dictyostelium* [49]. Considering that  
404 MYB64 is detectable in the pre-mitotic zygote and elevation of its transcription  
405 around mitosis in the synchronized cell culture (Fig. S5), MYB64 might also function  
406 during the M-phase. Admittedly, we do not have an appropriate experimental setup  
407 with live plants yet to test for a) if and how RBR controls *MYB64* during the M-phase  
408 in early zygotic development; and b) if two-repeat R2R3-type MYB64 plays a role in  
409 M-phase in the egg cell similar to what the three-repeat 3R-type MYBs do in other  
410 plant tissues [40]. In addition, a cell-cycle-independent function of both RBR and  
411 MYBs [13,22] from egg-to-zygote development will have to be investigated further.

412 It is also interesting to note that PRC2-specific repressive mark at the *MYB64* locus  
413 occurs in its gene body in the reproductive tissues, in contrast to the RBR-mediated  
414 repression of its promoter, indicating a rather complex regulation. Differential RBR  
415 binding between the two tested E2F binding sites in the *MYB64* promoter indicates  
416 its distinctive transcriptional regulation by RBR in reproductive versus sporophytic

417 development. We also found RBR binding to *LEC1* and *WOX2* promoters, perhaps  
418 along with the H3K27me3 mark, illustrating possible combined RBR-PRC2  
419 transcriptional regulation at their promoters during reproduction. Whereas *WOX2*  
420 seems to be directly repressed by RBR, and possibly also by the MYB64/119 and  
421 PRC2-mediated repression, RBR-MYBs function is necessary for maintaining *WOX8*  
422 expression. Together, RBR and MYB64/MYB119 play an important role in  
423 *WOX2/WOX8* balance in egg cell development, and probably also in ensuing zygote  
424 polarity establishment during the egg-to-zygotic reprogramming [8]. Therefore, RBR  
425 acts on promoters of a suite of transcription factors in the egg cell, while PRC2-  
426 dependent repression might play here an important parallel role. Cell-type specific  
427 data for the latter will have to be investigated in the future.

#### 428 **RBR network mediates egg cell development and stress responses thereof**

429 Previously, we have shown that the promoter activity of *RKD1* depends on intact  
430 RBR function in the egg cell [30]. Expression of *RKDs* and stress-related gene *LEC1*  
431 in the egg cell, a similar change of gene expression upon deregulation of RBR and  
432 MYB64/119 and upon stress, and their interaction with RBR, all indicate the  
433 underlying significance of this regulatory hub in plant reproduction. We propose that,  
434 unlike the RBR-MYB nodes described above, the network of RBR, *RKDs* and *LEC1*  
435 is likely cell cycle-independent, but associated with maintenance of cellular  
436 homeostasis and stress response. The cross-regulation within the *RKD* clade is  
437 intriguing. Whether it is RBR or MYB-mediated cellular stress and cell differentiation,  
438 or most abiotic stress types tested here, *RKD3* was activated but *RKD2* was  
439 downregulated. *RKD3* repression in the wild-type is likely connected to H3K27me3  
440 loading, and it is possible that RBR and PRC2 co-regulate this locus in a stress-

441 responsive manner, and this dual transcriptional control is similar to regulation of  
442 other genes during seed maturation and early seedling development [31].

443 Environmental stress is a major denominator of evolution of sex and germline  
444 throughout the Eukaryotes [50], and the land plants in particular evolved across  
445 gradients of limiting water and increasing light conditions [51]. Surprisingly, we found  
446 that RBR represses a subset of egg cell-expressed stress-related genes, supporting  
447 its role in reproductive stress amelioration. Therefore, the stress-associated RBR-  
448 MYB-RKD-LEC1-(PRC2) transcription factor network that we uncovered here  
449 features a prominent higher-order regulatory mechanism that may underlie egg cell  
450 development and homeostasis in plants.

#### 451 **Egg cell RBR network prevents parthenogenesis**

452 The twin egg cell-like development observed in both the *rbr* and *myb* double mutants  
453 suggest that both RBR and MYB64/MYB119 are likely factors involved in preventing  
454 cell proliferation in the egg cell domain and that their deregulation could serve as a  
455 prerequisite for parthenogenesis. It is interesting to note that downregulation of  
456 MSI1, a member of RBR and PRC2 complexes, triggers early events of  
457 parthenogenesis [12]. Dominant-negative approach shows that deregulation of *RKDs*  
458 leads to formation of twin eggs and rare parthenogenesis-like events, supported by  
459 recent findings of similar events observed in knock-outs and knock-ins of the  
460 corresponding evolutionary homolog in *Marchantia*, and down-regulation of a *RKD2*-  
461 like gene in unreduced egg cells of *Boechera* at the onset of parthenogenesis [51-  
462 53]. Whereas the role of LEC1 during sexual egg cell development is not known, it is  
463 a crucial embryonic factor, overexpression of which is sufficient to induce somatic  
464 embryogenesis [18]. Interestingly, along with increase of embryogenic *LEC1*

465 expression, abiotic stress induces abrogation of *RKD2*, *RKD3* derepression, and  
466 supernumerary egg production, supporting the general view that parthenogenesis  
467 evolved under stress conditions [54,55].

468 Combining genetic, transcription and protein interaction data, we propose a model  
469 for RBR-centric transcription factor network in the egg cell (Fig. 6), which integrates  
470 stress amelioration and cellular homeostasis as inherent aspects of successful egg  
471 cell development coordinated by a subset of transcription factors. The proposed  
472 RBR-centric regulatory model and the putative hierarchical RBR-centric protein  
473 interaction network for the egg cell (Fig. S6) might help to dissect further intricate  
474 regulatory mechanisms involving stress and development.

## 475 **Materials and Methods**

476 **Plant material.** Transgenic lines *rbr-3* [6,24], *myb64-4*, *myb119-1*, *pMYB64::MYB64-*  
477 *GFP* [13], *pLEC1::GUS* [35] were described previously

478 **Plasmid constructions.** For stable *in planta* transformations, we used following  
479 binary vectors containing L1-L2 Gateway® cassette, pK7WGF2 (VIB, Ghent) and  
480 p6N-GW (modified from the parent vector, DNA-Cloning-Service e.K., Hamburg).

481 *RBR* coding and gene/genomic sequences and *RKD2* genic sequences were PCR-  
482 amplified directly from *Arabidopsis* accession Col-0 cDNA/DNA and were prepared  
483 as Gateway entry clones, as per manufacturer's instructions (Thermo Fischer).

484 *RKD2<sup>DN</sup>* sequence was cloned as a hybrid *RKD2* gene fused to *EAR* sequences of  
485 the *SUPERMAN* locus, generating a *RKD2<sup>DN</sup>* entry clone. A 2.2 Kbp *RBR* promoter  
486 (or) 1.3 Kbp *RKD2* promoter, 550 bp *pECA1.1* PCR-amplicon were cloned into the  
487 binary vectors by DNA ligation using T4-DNA ligase (Thermo Fischer). For transient  
488 *in vivo* protein-protein interactions we used binary vector pGWB601 (Nakagawa

489 vectors, Addgene). For BiFC assembly, we used the *pUBI10*-driven Venus module  
490 sequences with very low self-assembly background signal described previously [56].  
491 Portal clones of Split-Venus partner pairs were stacked by our recently developed  
492 cloning system “Byepass”, which utilized bacterial and yeast based endogenous  
493 recombination; cloning and vector details are presented elsewhere [57].  
494 Terminal/binary clones were transformed into *Agrobacterium* via freeze-and-thaw  
495 method. Probes for *in situ* hybridization were PCR amplified as unique partial coding  
496 sequences of *MYB64*, *MYB119* and *EC1.1* from a cDNA pools from ovules, and  
497 cloned into an in-house expression vector.

498 **Plant selection, cultivation and transformation.** Surface-sterilized wild-type and  
499 transgenic seeds were germinated *in vitro* on MS half-strength plates without or with  
500 appropriate selection, subsequently transplanted into pots containing soil substrate,  
501 and cultivated in a long-day walk-in growth chamber conditions. Stable  
502 transformations of final agro-constructs were delivered into plants via floral-dip  
503 transformation [58]. A minimum of five independent transgenic lines were randomly  
504 chosen for genetic analysis of marker selection and seed set phenotyping; two  
505 representative lines were chosen for further analysis. Transient transformation of  
506 tobacco leaf mesophyll cells was achieved by *Agrobacterium*-mediated infiltration, as  
507 explained previously [59].

508 **Abiotic stress induction.** Stress treatments were given to soil-grown *Arabidopsis*  
509 plants. Flowering plants were exposed to stress conditions for one week before  
510 collection of pistils/ovules for down-stream analyses. For salt treatment, plants/pots  
511 were watered with 100mM NaCl every two days at 22°C; for elevated temperature  
512 treatment plants were placed at 27°C with sufficient watering; for drought treatment

513 plants were minimally watered upon first signs of wilting at 22°C; control conditions  
514 were 22°C with normal watering regime every two days.

515 **BiFC.** Bimolecular Fluorescent Complementation assay was performed in young  
516 tobacco leaves upon transient agrobacterium-mediated transformation of BiFC  
517 constructs. RBR was fused at its N-terminus to C-Venus, and the tested interactors  
518 with N-Venus [56]. As negative controls, we used empty BiFC vector pair as well as  
519 C-Ven-RBR with empty N-Ven. Both combinations did not show meaningful  
520 fluorescence, as expected in BiFC experiments that used the improved parent  
521 vectors [56].

522 **Microscopy.** Fixed samples cleared in chloral hydrate for clearing analyses and/or  
523 those histochemically-stained for GUS detection [6] were observed under a Leica  
524 DMI6000 inverted microscope (Leica Microsystems) fitted with an Orca 4 camera  
525 (Hamamatsu). GUS staining was performed as in [22]. Confocal microscopy of  
526 Feulgen-stained samples [22] and/or live fluorescent samples were analysed under  
527 Zeiss LSM 780 (Carl Zeiss) or Leica SP8 (Leica Microsystems) confocal scanning  
528 laser microscopy platforms.

529 **mRNA *in situ* hybridization** was performed as described earlier [22]. Probes were  
530 prepared by *in vitro* transcription of appropriate template plasmids, and were  
531 hybridized on to 8 µm semi-thin sections of emasculated pistils containing mature  
532 ovules.

533 **RNA extraction and cDNA synthesis.** Minute ovule samples were pre-fixed in  
534 ethanol as described earlier [60] for all RT-PCR except for RNA-seq analysis ovules  
535 were scrapped out and snap-frozen immediately. It is important to note that the *rbr-3*  
536 mutant is homozygous lethal; therefore, plants heterozygous for *rbr-3* ubear only

537 50% ovules with haploid *rbr-3* embryo sacs that are encased by diploid integuments  
538 heterozygous for the same mutation [6,22,24]. *rbr-3* ovules were hand-picked as  
539 described in [28]. *myb64;myb119* ovules were pooled from homo-heterozygous  
540 double mutant plants [13]. Frozen tissues were ground in a tissue lyser (QiAgen),  
541 and the total RNA was prepared using RNA-Aqueous Micro kit and/or Trizol (Thermo  
542 Fischer), as per manufacturer's instructions. Reverse transcription was performed on  
543 DNase I-treated samples using SuperScript IV First-Strand Synthesis System  
544 (Thermo Fischer).

545 **mRNA-seq libraries and sequencing.** Total RNA extracted from ovules of WT and  
546 mutant was quality-checked in a Bioanalyzer (Thermo Fischer). Purification of  
547 transcripts, library preparation and NGS sequencing were performed in a sequencing  
548 facility according to the routine pipeline (Fasteris, Switzerland). Paired-end  
549 sequencing generated approximately 100 bp per read in an Illumina HiSeq2000  
550 platform.

551 **Expression analysis based on mRNA-seq.** The quality of raw reads was assessed  
552 using FastQC [61]. RNAseq samples from wild-type and *rbr-3/+* mature ovules were  
553 aligned to the *Arabidopsis* TAIR10 reference genome using Bowtie2 [62] with  
554 settings for sensitive mode. The number of uniquely mapped reads to each gene  
555 described in the reference genome annotation release of Araport11 [63] were  
556 counted using HTSeq [64]. Transcripts that were significantly differently expressed  
557 between wild-type and *rbr-3/+* ovules were identified using the NOISeq pipeline at a  
558 threshold of  $q > 0.95$  [65]. The egg cell specific transcriptome between the wild-type  
559 and *rbr* mutant was derived from the overlap between the expressed transcripts in  
560 the wild-type and *rbr-3/+* ovules and the transcripts reported in a previous microarray



561 from the egg cells [9]. Gene ontology (GO) enrichment analysis was done using  
562 BINGO [66] and visualized with Cytoscape [67].

563 **LexA-based yeast-two-hybrid growth assay** with RBR CDS was performed  
564 according to standard protocols. In brief, full-length coding sequences were cloned  
565 into modified pGilda bait (RBR) with 202-residue LexA domain, and pB24AD prey  
566 vectors (MATCHMAKER LexA Two-Hybrid System, Clontech), and transformed into  
567 high sensitivity yeast strain EGY48. Interactions were tested on synthetic complete  
568 (SC) yeast medium agar plates barring UHTL (Uracil, Histidine, Threonine, Leucine).

569 **Protein interaction network analysis.** Protein interaction network with egg cell  
570 enriched transcripts, transcription factor and down-stream stress related transcripts  
571 was created and visualized using GeneMANIA [68] and Cytoscape [67]. The primary  
572 networks were manually processed to remove non-significant and low confidence  
573 interactions to keep the network that had only physical and predicted interactions.  
574 Single nodes that did not have a direct link to RBR were removed, and the network  
575 was cropped to include the first node that linked RBR with a known stress associated  
576 protein. Additional links that created subnetworks from stress associated proteins  
577 included in the core network were also removed as these subnetworks did not add  
578 new information to link RBR to stress responses.

579 RBR and other interacting transcription factors are organized at the center followed  
580 by stress responsive genes at the outermost circle. The novel physical connections  
581 between RBR, MYB64, LEC1 and RKDs, discovered in the current study are shown  
582 in solid dark brown lines. The solid gray lines indicate published physical protein-  
583 protein interactions and the gray dashed-lines indicate published predicted protein-  
584 protein interactions. The intensity of the lines represents the significance of the

585 interactions such as multiple independent studies. The white nodes represent  
586 proteins found to interact in published networks, but not enriched as transcripts in the  
587 deduced *rbr-3* egg cell transcriptome.

588 **H3K27 trimethylation target identification.** H3K27 trimethylation targets for the  
589 *Arabidopsis* flower tissues were obtained from the plantDHS database [69].

590 Upstream regions of the genes of interest in *Arabidopsis* genome [63] were searched  
591 at different window lengths to identify H3K27me3 targets. Finally, methylation targets  
592 in 500 upstream windows of the transcription start site (TSS) were reported as  
593 H3K27 trimethylation targets concentrated within this region.

594 **Chromatin immuno-precipitation (ChIP).** RBR ChIP was performed on plants  
595 carrying *pRBR::GFP-RBR* in *rbr-3* background, *pEC::tagRFP-RBR*, and H3K27me3  
596 ChIP on wild-type Col-0 plants. 3-week-old wild-type and *GFP-gRBR* seedlings, wild-  
597 type and *pRBR::GFP-RBR* inflorescences containing buds and open flowers before  
598 fertilization and gynoecia of wild-type and *pEC::tagRFP-RBR* unfertilized open  
599 flowers containing mature egg cells were collected. Egg-cell-targeted RBR ChIP was  
600 performed only for validation of a few fragments, as collection of material is  
601 extremely tedious and gynoecia contain a small proportion of egg cells resulting in a  
602 very low amount of bound DNA. Due to technical limitations in large-scale isolation of  
603 single egg cells required for H3K27me3 ChIP experiments, it was not possible to  
604 disentangle egg cell histone methylation patterns from the surrounding reproductive  
605 sporophytic tissues; therefore, we used mature unfertilized gynoecia. ChIP  
606 experiments were performed accordingly to the X-ChIP protocol as described in [59]  
607 using anti-GFP (Abcam, ab290), anti-RFP (AbCam, ab62341), anti-H3K27me3  
608 (Millipore, #07-449) and anti-IgG (Abcam, ab6703) antibody.

609 **Real-time qPCR.** Both for RT-qPCR or ChIP-qPCR applications, SYBR Green  
610 assays were performed in QuantStudio5 Real-Time-PCR System (Thermo Fischer).  
611 A minimum of three biological replicates and two technical replicates were used in  
612 the experiments. The RT-qPCR data were normalized for expression of UBX  
613 domain-containing protein, *AT4G10790* [70]. For ChIP-qPCR, the values were  
614 normalized by the input, and background subtraction was performed for anti-GFP  
615 ChIP. Quantification of relative gene expression or DNA enrichment, and analyses of  
616 statistical inference using Student-t test were performed in Microsoft Excel 2010.

617 **Statistical analysis:** Fisher`s exact test

618 <http://graphpad.com/quickcalcs/contingency2/>

619

620 **ACKNOWLEDGMENTS.** Acknowledged are funding from German Research  
621 Foundation (Emmy-Noether grant JO1001/1-1, DFG) and the Baden-Wuerttemberg  
622 State (LGFG) to A.J.J., the Max-Planck Society to F.T., National Science Foundation  
623 (NSF) to M.D, and Swiss National Science Foundation to W.G. We thank Gary  
624 Drews (University of Utah, USA) for kindly sharing transgenic material and advice,  
625 Claudia Casalongué (National University of Mar del Plata, Argentina) and Johan  
626 Peränen (University of Helsinki, Finland) for sharing yeast vectors, Marlene Zimmer  
627 (Heidelberg University) and Petra Tänzler (MPI Cologne) for technical help, Nora  
628 Mueller, Anika Rütz and Muhammad Tayyab (Heidelberg University) for help with  
629 cloning and plant work, Juan Mateo (University of Oviedo, Spain) for helpful  
630 suggestions regarding RNA-seq. Ivana Mesic and Claudia Sas (Thermo Scientific)  
631 for advice on real-time qPCR. We thank Nottingham Arabidopsis Stock Centre  
632 (NASC) for distributing transgenic seeds. Thanks are due to Sureshkumar

633 Balasubramanian (Monash University, Australia) for critical comments on the  
634 manuscript.

635

### 636 **Author Contributions**

637 A.J.J. designed and supervised the research. O.K., Pa.P., G.G., R.L., V.N, D.S.L.,  
638 A.M.R., P.v.B. performed research. F.T. provided additional reagents and supervised  
639 specific experiments; O.K., Pr.P., J.S., C.W., Y.Z., W.G., F.T., M.D. and A.J.J.  
640 analysed data; M.D. supervised bioinformatic analysis; O.K. and A.J.J. wrote the  
641 paper with inputs from co-authors.

642

643

644

645 **Fig. 1. RBR-MYB transcription factors are essential for faithful egg cell**  
646 **development. (A)** Rescue of ovule/seed abortion in *rbr-3* plants in presence of the  
647 two RBR constructs. **(B)** Transmission of *rbr-3* allele to the progeny in presence of  
648 three tagged RBR constructs, scored by resistance to Sulfadiazine (Sul, S -  
649 sensitive; R- resistant). **(C)** eGFP fused to genomic RBR is detectable in the mature  
650 egg cell. **(D)** GFP-gRBR signal is largely depleted in the polarized zygote upon  
651 fertilization (~8 hours after pollination, hap). **(E)** Quantification of GFP-RBR signals  
652 before and after fertilization (BF, AF). **(F)** Egg cell-specific tagging of RBR by  
653 *tagRFP-RBR* fusion. **(G-H)** Feulgen-stained female gametophytes: **(G)** A mature  
654 wild-type (WT) embryo sac showing an egg and other cell types such as two  
655 synergids and a central cell. **(H)** Loss of *MYB64/MYB119* leads to embryo sac  
656 proliferation. **(I)** MYB64-GFP protein in the mature egg cell. **(J)** MYB64-GFP upon  
657 pollen tube entry (~8 hap). **(K)** MYB64-GFP signals quantified. **(L)** RKD2-GUS  
658 translational fusion is localized to the egg cell only. **(M)** *pLEC1-GUS* is faintly  
659 expressed in the mature egg cell-containing embryo sac. Red/green/blue/white  
660 arrow-heads: egg/synergids/sperm/central cell. Scale bar=20µm.

661

662 **Fig. 2. Abrogation of RBR causes global egg cell-expressed gene deregulation.**

663 **(A)** A schematic of ovule samples used for differential RNA-seq analysis. **(B)** Genetic  
664 subtraction of egg cell-expressed genes from the ovule transcripts identifies genes  
665 regulated by RBR in the egg cells. **(C,F,G)** Validation of RBR-regulated candidate  
666 genes by real-time qRT-PCR in *rbr-3*, and testing in *myb64;myb119* ovules.  
667 Significance  $**\alpha \leq 0.01$ ;  $*\alpha \leq 0.05$ . **(D-E)** Spatial validation of RBR-regulated *EC1.1*  
668 by mRNA *in situ* hybridization.

669

670 **Fig. 3. RBR associates with gene promoters of MYB and RKD families of**  
671 **transcription factors. (A)** Location of RBR protein interaction with DNA fragments  
672 tested in Chromatin-Immunoprecipitation for RBR or for the PRC2-specific  
673 H3K27me3. **(B-C)** ChIP in reproductive tissues containing mature egg cells. Relative  
674 ChIP-qPCR normalized by input. Significant difference between the negative control  
675 (background) and the experimental values: \*\* $\alpha \leq 0.01$ ; \* $\alpha \leq 0.05$ .

676

677 **Fig. 4. Abiotic stress and deregulation of RBR network leads to additional egg**  
678 **cells. (A)** A WT embryo sac with mature egg cell. **(B-D)** Supernumerary eggs in *rbr-*  
679 *3* and *myb64;myb119*, and *pEC::RKD<sup>DN</sup>* embryo sacs. **(E)** A *pEC::RKD<sup>DN</sup>* ovule with  
680 rare three egg cell-like phenotype or completely collapsed **(F)**. **(G)** A sexual zygote in  
681 WT at ~12 hap. **(H-I)** rare fertilization-independent zygote-like structure or  
682 parthenogenetic embryo in *pEC::RKD<sup>DN</sup>* ovules 6 days after emasculation. **(J-M)**  
683 salt-stress induced embryo sac defects and twin eggs. **(N)** WT-looking drought-  
684 treated ovule. **(P-U)** *LEC1* expression in the embryo sac under salt stress (Q),  
685 elevated temperature (27°C) (R), and drought (S). *LEC1* is activated in the synergid  
686 upon pollen tube entry ~ 6 hap (T), and only residual *LEC1* is detectable when the  
687 zygote is polarized a day after pollination (U). Scale bar = 20 $\mu$ m. hap – hours after  
688 pollination. See Fig. 1 for color-scheme of arrow-heads, brown – collapsing embryo  
689 sac; yellow – suspensor. **(V)** Relative expression in mature egg cell-containing  
690 gynoecia under stress. Significance \*\* $\alpha \leq 0.01$ ; \* $\alpha \leq 0.05$

691

692

693 **Fig. 5. RBR physically interacts with MYB and RKD families of transcription**  
694 **factors. (A)** Transient BiFC assay. RBR-MSI1 pair was used as a positive control  
695 [28], self-assembly of split-Venus as a negative control. **(B)** Quantification of BiFC  
696 interaction strength. Relative YFP fluorescence intensity in nuclei with background  
697 subtraction. C-Ven-RBR was tested with the respective N-Ven-protein fusions. Empty split  
698 Venus pair was used as a control in order to monitor unspecific background signals.

699

700 **Fig. 6. A model of cross-regulation between a subset of RBR-regulated**  
701 **transcription factors in the *Arabidopsis* egg cells.** Illustrated is a schematic view  
702 of how interacting proteins RBR and MYBs-commonly regulate a subset of  
703 transcription factor-encoding genes expressed in the egg cell. RBR/MYBs repress  
704 transcription of egg cell-specific *RKD3* and *WOX2*, and activate *RKD2* and *WOX8*.  
705 RBR/MYB repress egg cell-expressed stress response genes, in particular *LEC1*,  
706 indicating their role in cellular homeostasis. RBR may mediate gene repression in  
707 concert with PRC2-specific repressive H3K27me3 mark.

- 708 1. Tekleyohans DG, Nakel T, Gross-Hardt R (2017) Patterning the Female Gametophyte of  
709 Flowering Plants. *Plant Physiol* 173: 122-129.
- 710 2. Johnston AJ, Meier P, Gheyselinck J, Wuest SE, Federer M, et al. (2007) Genetic  
711 subtraction profiling identifies genes essential for Arabidopsis reproduction and  
712 reveals interaction between the female gametophyte and the maternal sporophyte.  
713 *Genome Biol* 8: R204.
- 714 3. Kirioukhova O, Johnston AJ, Kleen D, Kagi C, Baskar R, et al. (2011) Female  
715 gametophytic cell specification and seed development require the function of the  
716 putative Arabidopsis INCENP ortholog WYRD. *Development* 138: 3409-3420.
- 717 4. Kong J, Lau S, Jurgens G (2015) Twin plants from supernumerary egg cells in  
718 Arabidopsis. *Curr Biol* 25: 225-230.
- 719 5. Bencivenga S, Colombo L, Masiero S (2011) Cross talk between the sporophyte and the  
720 megagametophyte during ovule development. *Sex Plant Reprod* 24: 113-121.
- 721 6. Johnston AJ, Matveeva E, Kirioukhova O, Grossniklaus U, Grissem W (2008) A dynamic  
722 reciprocal RBR-PRC2 regulatory circuit controls Arabidopsis gametophyte  
723 development. *Curr Biol* 18: 1680-1686.
- 724 7. Kimata Y, Higaki T, Kawashima T, Kurihara D, Sato Y, et al. (2016) Cytoskeleton  
725 dynamics control the first asymmetric cell division in Arabidopsis zygote. *Proc Natl*  
726 *Acad Sci U S A* 113: 14157-14162.
- 727 8. Ueda M, Zhang Z, Laux T (2011) Transcriptional activation of Arabidopsis axis patterning  
728 genes WOX8/9 links zygote polarity to embryo development. *Dev Cell* 20: 264-270.
- 729 9. Wuest SE, Vijverberg K, Schmidt A, Weiss M, Gheyselinck J, et al. (2010) Arabidopsis  
730 female gametophyte gene expression map reveals similarities between plant and  
731 animal gametes. *Curr Biol* 20: 506-512.
- 732 10. Anderson SN, Johnson CS, Jones DS, Conrad LJ, Gou X, et al. (2013) Transcriptomes of  
733 isolated *Oryza sativa* gametes characterized by deep sequencing: evidence for distinct  
734 sex-dependent chromatin and epigenetic states before fertilization. *Plant J* 76: 729-  
735 741.
- 736 11. Conner JA, Mookkan M, Huo H, Chae K, Ozias-Akins P (2015) A parthenogenesis gene  
737 of apomict origin elicits embryo formation from unfertilized eggs in a sexual plant.  
738 *Proc Natl Acad Sci U S A* 112: 11205-11210.
- 739 12. Guitton AE, Berger F (2005) Loss of function of MULTICOPY SUPPRESSOR OF IRA  
740 1 produces nonviable parthenogenetic embryos in Arabidopsis. *Curr Biol* 15: 750-  
741 754.
- 742 13. Rabiger DS, Drews GN (2013) MYB64 and MYB119 are required for cellularization and  
743 differentiation during female gametogenesis in Arabidopsis thaliana. *PLoS Genet* 9:  
744 e1003783.
- 745 14. Horstman A, Li M, Heidmann I, Weemen M, Chen B, et al. (2017) The BABY BOOM  
746 Transcription Factor Activates the LEC1-ABI3-FUS3-LEC2 Network to Induce  
747 Somatic Embryogenesis. *Plant Physiol* 175: 848-857.
- 748 15. Zuo J, Niu QW, Frugis G, Chua NH (2002) The WUSCHEL gene promotes vegetative-  
749 to-embryonic transition in Arabidopsis. *Plant J* 30: 349-359.
- 750 16. Wang X, Niu QW, Teng C, Li C, Mu J, et al. (2009) Overexpression of PGA37/MYB118  
751 and MYB115 promotes vegetative-to-embryonic transition in Arabidopsis. *Cell Res*  
752 19: 224-235.
- 753 17. Pelletier JM, Kwong RW, Park S, Le BH, Baden R, et al. (2017) LEC1 sequentially  
754 regulates the transcription of genes involved in diverse developmental processes  
755 during seed development. *Proc Natl Acad Sci U S A*.



- 756 18. West M, Yee KM, Danao J, Zimmerman JL, Fischer RL, et al. (1994) LEAFY  
757 COTYLEDON1 Is an Essential Regulator of Late Embryogenesis and Cotyledon  
758 Identity in Arabidopsis. *Plant Cell* 6: 1731-1745.
- 759 19. Pillot M, Autran D, Leblanc O, Grimanelli D (2010) A role for  
760 CHROMOMETHYLASE3 in mediating transposon and euchromatin silencing during  
761 egg cell reprogramming in Arabidopsis. *Plant Signal Behav* 5: 1167-1170.
- 762 20. She W, Baroux C (2014) Chromatin dynamics during plant sexual reproduction. *Front*  
763 *Plant Sci* 5: 354.
- 764 21. Friedman WE (1999) Expression of the cell cycle in sperm of Arabidopsis: implications  
765 for understanding patterns of gametogenesis and fertilization in plants and other  
766 eukaryotes. *Development* 126: 1065-1075.
- 767 22. Johnston AJ, Kirioukhova O, Barrell PJ, Rutten T, Moore JM, et al. (2010) Dosage-  
768 sensitive function of retinoblastoma related and convergent epigenetic control are  
769 required during the Arabidopsis life cycle. *PLoS Genet* 6: e1000988.
- 770 23. Ingouff M, Sakata T, Li J, Sprunck S, Dresselhaus T, et al. (2009) The two male gametes  
771 share equal ability to fertilize the egg cell in Arabidopsis thaliana. *Curr Biol* 19: R19-  
772 20.
- 773 24. Ebel C, Mariconti L, Gruissem W (2004) Plant retinoblastoma homologues control  
774 nuclear proliferation in the female gametophyte. *Nature* 429: 776-780.
- 775 25. Gutzat R, Borghi L, Gruissem W (2012) Emerging roles of RETINOBLASTOMA-  
776 RELATED proteins in evolution and plant development. *Trends Plant Sci* 17: 139-  
777 148.
- 778 26. Harashima H, Sugimoto K (2016) Integration of developmental and environmental  
779 signals into cell proliferation and differentiation through RETINOBLASTOMA-  
780 RELATED 1. *Curr Opin Plant Biol* 29: 95-103.
- 781 27. Sprunck S, Rademacher S, Vogler F, Gheyselinck J, Grossniklaus U, et al. (2012) Egg  
782 cell-secreted EC1 triggers sperm cell activation during double fertilization. *Science*  
783 338: 1093-1097.
- 784 28. Jullien PE, Mosquna A, Ingouff M, Sakata T, Ohad N, et al. (2008) Retinoblastoma and  
785 its binding partner MSI1 control imprinting in Arabidopsis. *PLoS Biol* 6: e194.
- 786 29. Haecker A, Gross-Hardt R, Geiges B, Sarkar A, Breuninger H, et al. (2004) Expression  
787 dynamics of WOX genes mark cell fate decisions during early embryonic patterning  
788 in Arabidopsis thaliana. *Development* 131: 657-668.
- 789 30. Koszegi D, Johnston AJ, Rutten T, Czihal A, Altschmied L, et al. (2011) Members of the  
790 RKD transcription factor family induce an egg cell-like gene expression program.  
791 *Plant J* 67: 280-291.
- 792 31. Gutzat R, Borghi L, Futterer J, Bischof S, Laizet Y, et al. (2011) RETINOBLASTOMA-  
793 RELATED PROTEIN controls the transition to autotrophic plant development.  
794 *Development* 138: 2977-2986.
- 795 32. Tedeschi F, Rizzo P, Rutten T, Altschmied L, Baumlein H (2017) RWP-RK domain-  
796 containing transcription factors control cell differentiation during female gametophyte  
797 development in Arabidopsis. *New Phytol* 213: 1909-1924.
- 798 33. Jeong S, Palmer TM, Lukowitz W (2011) The RWP-RK factor GROUNDED promotes  
799 embryonic polarity by facilitating YODA MAP kinase signaling. *Curr Biol* 21: 1268-  
800 1276.
- 801 34. Hiratsu K, Matsui K, Koyama T, Ohme-Takagi M (2003) Dominant repression of target  
802 genes by chimeric repressors that include the EAR motif, a repression domain, in  
803 Arabidopsis. *Plant J* 34: 733-739.

- 804 35. Siefers N, Dang KK, Kumimoto RW, Bynum WEt, Tayrose G, et al. (2009) Tissue-  
805 specific expression patterns of Arabidopsis NF-Y transcription factors suggest  
806 potential for extensive combinatorial complexity. *Plant Physiol* 149: 625-641.
- 807 36. Friend SH, Bernards R, Rogelj S, Weinberg RA, Rapaport JM, et al. (1986) A human  
808 DNA segment with properties of the gene that predisposes to retinoblastoma and  
809 osteosarcoma. *Nature* 323: 643-646.
- 810 37. Takemura M (2005) Evolutionary history of the retinoblastoma gene from archaea to  
811 eukarya. *Biosystems* 82: 266-272.
- 812 38. Lipsick JS (2010) The C-MYB story--is it definitive? *Proc Natl Acad Sci U S A* 107:  
813 17067-17068.
- 814 39. Guiley KZ, Liban TJ, Felthousen JG, Ramanan P, Litovchick L, et al. (2015) Structural  
815 mechanisms of DREAM complex assembly and regulation. *Genes Dev* 29: 961-974.
- 816 40. Kobayashi K, Suzuki T, Iwata E, Nakamichi N, Chen P, et al. (2015) Transcriptional  
817 repression by MYB3R proteins regulates plant organ growth. *EMBO J* 34: 1992-  
818 2007.
- 819 41. Fischer M, Grossmann P, Padi M, DeCaprio JA (2016) Integration of TP53, DREAM,  
820 MMB-FOXM1 and RB-E2F target gene analyses identifies cell cycle gene regulatory  
821 networks. *Nucleic Acids Res* 44: 6070-6086.
- 822 42. Stracke R, Werber M, Weisshaar B (2001) The R2R3-MYB gene family in Arabidopsis  
823 thaliana. *Curr Opin Plant Biol* 4: 447-456.
- 824 43. Nakajima Y, Yamada S, Kamata N, Ikeda MA (2007) Interaction of E2F-Rb family  
825 members with corepressors binding to the adjacent E2F site. *Biochem Biophys Res*  
826 *Commun* 364: 1050-1055.
- 827 44. Sala A, De Luca A, Giordano A, Peschle C (1996) The retinoblastoma family member  
828 p107 binds to B-MYB and suppresses its autoregulatory activity. *J Biol Chem* 271:  
829 28738-28740.
- 830 45. Yang QE, Nagaoka SI, Gwost I, Hunt PA, Oatley JM (2015) Inactivation of  
831 Retinoblastoma Protein (Rb1) in the Oocyte: Evidence That Dysregulated Follicle  
832 Growth Drives Ovarian Teratoma Formation in Mice. *PLoS Genet* 11: e1005355.
- 833 46. Menges M, Hennig L, Gruissem W, Murray JA (2003) Genome-wide gene expression in  
834 an Arabidopsis cell suspension. *Plant Mol Biol* 53: 423-442.
- 835 47. Lam EW, Bennett JD, Watson RJ (1995) Cell-cycle regulation of human B-myb  
836 transcription. *Gene* 160: 277-281.
- 837 48. DeFilippis RA, Goodwin EC, Wu L, DiMaio D (2003) Endogenous human  
838 papillomavirus E6 and E7 proteins differentially regulate proliferation, senescence,  
839 and apoptosis in HeLa cervical carcinoma cells. *J Virol* 77: 1551-1563.
- 840 49. Strasser K, Bloomfield G, MacWilliams A, Ceccarelli A, MacWilliams H, et al. (2012) A  
841 retinoblastoma orthologue is a major regulator of S-phase, mitotic, and developmental  
842 gene expression in Dictyostelium. *PLoS One* 7: e39914.
- 843 50. Maklakov AA, Immler S (2016) The Expensive Germline and the Evolution of Ageing.  
844 *Curr Biol* 26: R577-586.
- 845 51. Koi S, Hisanaga T, Sato K, Shimamura M, Yamato KT, et al. (2016) An Evolutionarily  
846 Conserved Plant RKD Factor Controls Germ Cell Differentiation. *Curr Biol* 26: 1775-  
847 1781.
- 848 52. Rovekamp M, Bowman JL, Grossniklaus U (2016) Marchantia MpRKD Regulates the  
849 Gametophyte-Sporophyte Transition by Keeping Egg Cells Quiescent in the Absence  
850 of Fertilization. *Curr Biol* 26: 1782-1789.
- 851 53. Schmidt A, Schmid MW, Klostermeier UC, Qi W, Guthorl D, et al. (2014) Apomictic and  
852 sexual germline development differ with respect to cell cycle, transcriptional,  
853 hormonal and epigenetic regulation. *PLoS Genet* 10: e1004476.

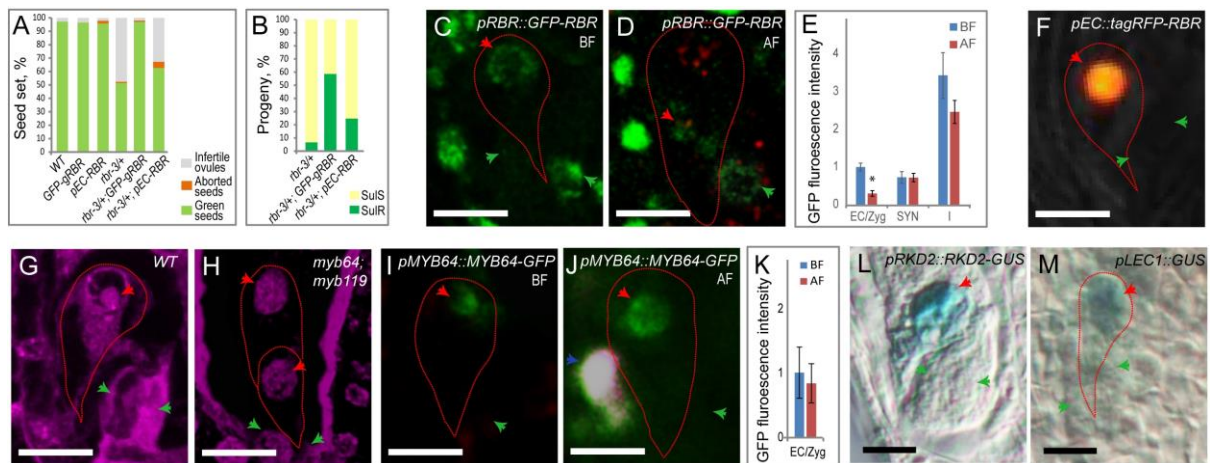
- 854 54. Hand ML, de Vries S, Koltunow AM (2016) A Comparison of In Vitro and In Vivo  
855 Asexual Embryogenesis. *Methods Mol Biol* 1359: 3-23.
- 856 55. Shah JN, Kirioukhova O, Pawar P, Tayyab M, Mateo JL, et al. (2016) Depletion of Key  
857 Meiotic Genes and Transcriptome-Wide Abiotic Stress Reprogramming Mark Early  
858 Preparatory Events Ahead of Apomeiotic Transition. *Front Plant Sci* 7: 1539.
- 859 56. Gookin TE, Assmann SM (2014) Significant reduction of BiFC non-specific assembly  
860 facilitates in planta assessment of heterotrimeric G-protein interactors. *Plant J* 80:  
861 553-567.
- 862 57. Kirioukhova O, Rhahul AM, Pawar P, Begum J, Venkatesh M, et al. (submitted) A robust  
863 and versatile homology-(in)dependent multi-fragment assembly for functional  
864 transgenesis.
- 865 58. Clough SJ, Bent AF (1998) Floral dip: a simplified method for *Agrobacterium*-mediated  
866 transformation of *Arabidopsis thaliana*. *Plant J* 16: 735-743.
- 867 59. Zhou Y, Tergemina E, Cui H, Forde A, Hartwig B, et al. (2017) Ctf4-related protein  
868 recruits LHP1-PRC2 to maintain H3K27me3 levels in dividing cells in *Arabidopsis*  
869 *thaliana*. *Proc Natl Acad Sci U S A* 114: 4833-4838.
- 870 60. Steffen JG, Kang IH, Macfarlane J, Drews GN (2007) Identification of genes expressed in  
871 the *Arabidopsis* female gametophyte. *Plant J* 51: 281-292.
- 872 61. Andrews S (2010) FastQC: a quality control tool for high throughput sequence data.  
873 <http://www.bioinformaticsbabraham.ac.uk/projects/fastqc>.
- 874 62. Langmead B, Salzberg SL (2012) Fast gapped-read alignment with Bowtie 2. *Nat*  
875 *Methods* 9: 357-359.
- 876 63. Cheng CY, Krishnakumar V, Chan AP, Thibaud-Nissen F, Schobel S, et al. (2017)  
877 *Araport11*: a complete reannotation of the *Arabidopsis thaliana* reference genome.  
878 *Plant J* 89: 789-804.
- 879 64. Anders S, Pyl PT, Huber W (2015) HTSeq--a Python framework to work with high-  
880 throughput sequencing data. *Bioinformatics* 31: 166-169.
- 881 65. Tarazona S, Furio-Tari P, Turra D, Pietro AD, Nueda MJ, et al. (2015) Data quality aware  
882 analysis of differential expression in RNA-seq with NOISeq R/Bioc package. *Nucleic*  
883 *Acids Res* 43: e140.
- 884 66. Maere S, Heymans K, Kuiper M (2005) BiNGO: a Cytoscape plugin to assess  
885 overrepresentation of gene ontology categories in biological networks. *Bioinformatics*  
886 21: 3448-3449.
- 887 67. Shannon P, Markiel A, Ozier O, Baliga NS, Wang JT, et al. (2003) Cytoscape: a software  
888 environment for integrated models of biomolecular interaction networks. *Genome Res*  
889 13: 2498-2504.
- 890 68. Mostafavi S, Ray D, Warde-Farley D, Grouios C, Morris Q (2008) GeneMANIA: a real-  
891 time multiple association network integration algorithm for predicting gene function.  
892 *Genome Biol* 9 Suppl 1: S4.
- 893 69. Zhang T, Marand AP, Jiang J (2016) PlantDHS: a database for DNase I hypersensitive  
894 sites in plants. *Nucleic Acids Res* 44: D1148-1153.
- 895 70. Kudo T, Sasaki Y, Terashima S, Matsuda-Imai N, Takano T, et al. (2016) Identification  
896 of reference genes for quantitative expression analysis using large-scale RNA-seq  
897 data of *Arabidopsis thaliana* and model crop plants. *Genes Genet Syst* 91: 111-125.

898

899

900

901



902

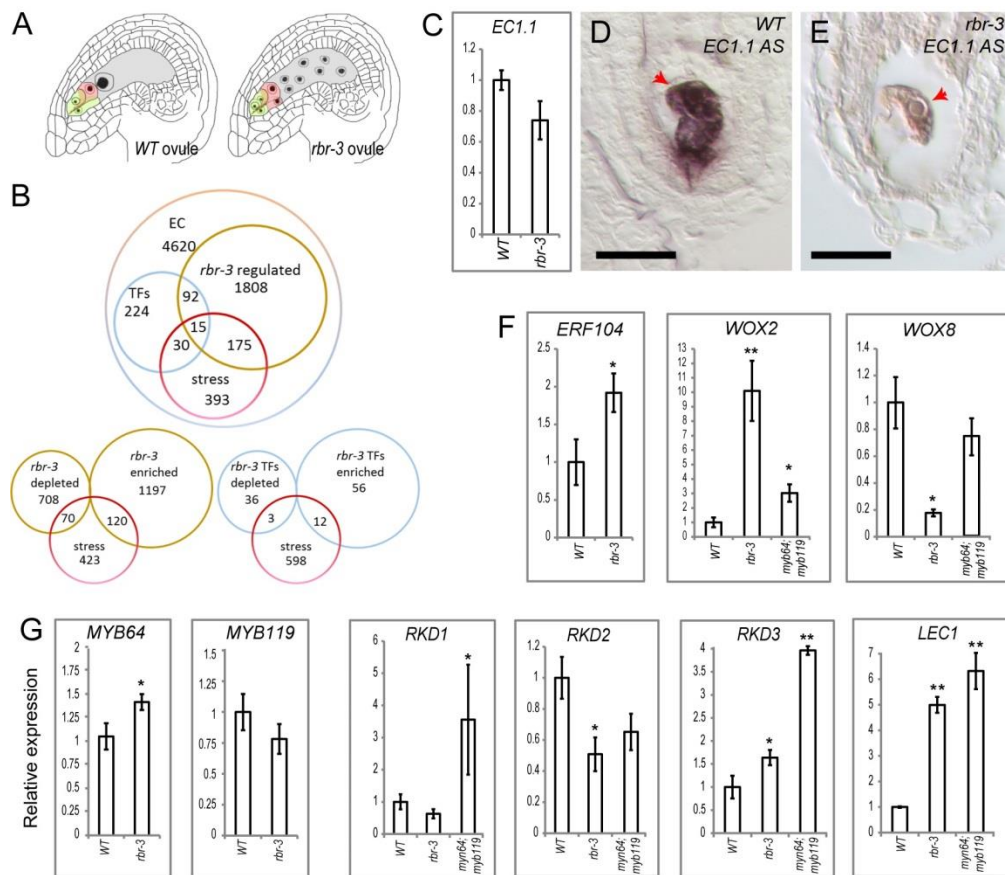
903 Fig. 1

904

905

906

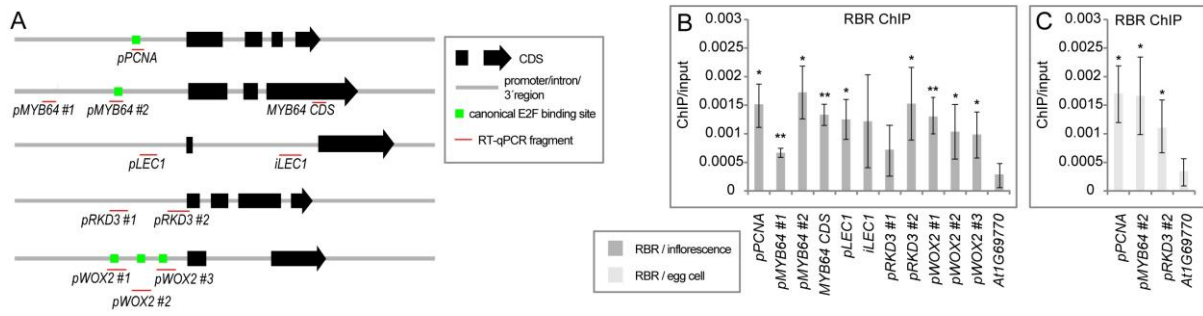
907



908

909 Fig. 2

910



911

912

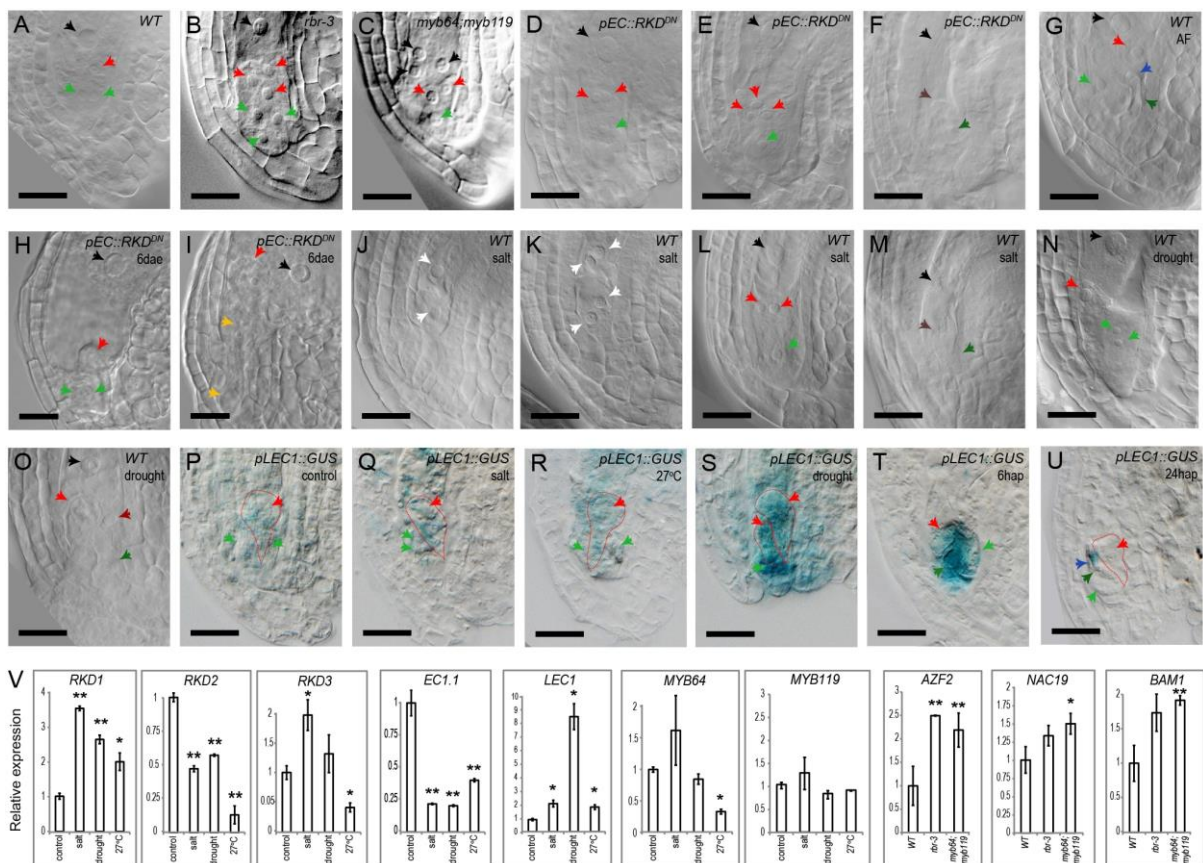
913 Fig. 3

914

915

916

917



918

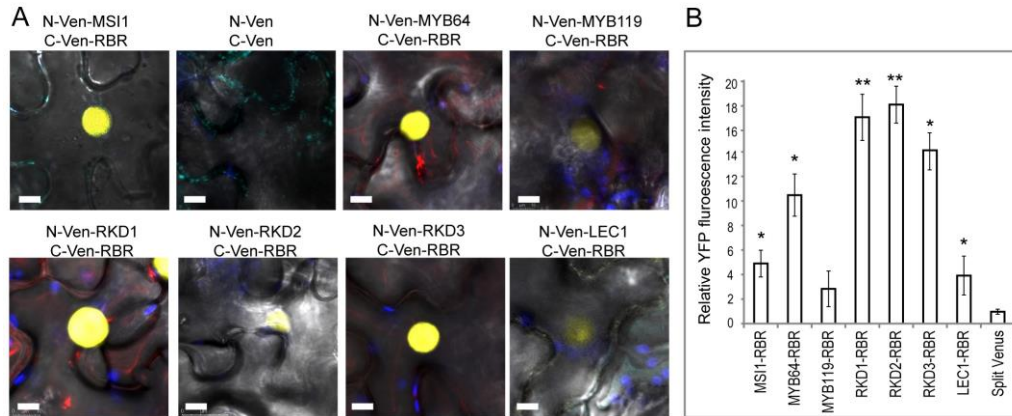
919 Fig. 4

920

921

922

923



924

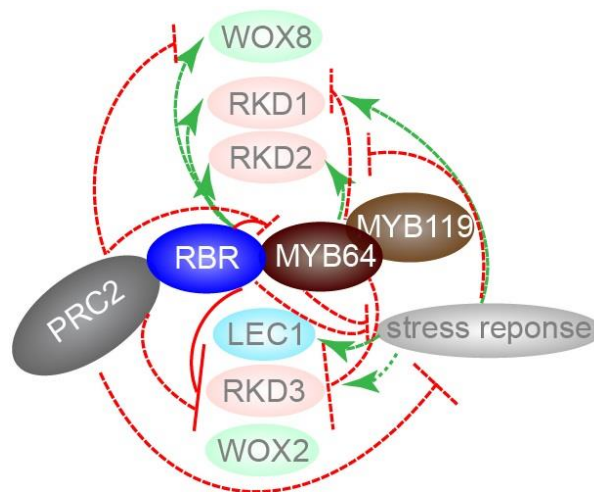
925 Fig. 5

926

927

928

929



930

931 Fig. 6

932

933 **Supporting Information**

934

935 **Table S1. A hemizygous transgene *GFP-gRBR* fully restores fertility of *rbr-3***  
936 **gametophytes in *rbr-3/RBR; GFP-gRBR<sup>h</sup>*.**

937 **Table S2. Progeny test confirms ‘two independent loci’ complementation of**  
938 ***rbr-3* allele with *GFP-gRBR* in *rbr-3/RBR; GFP-gRBR<sup>h</sup>* background. Note that**  
939 **offspring was scored based on antibiotic resistance of *rbr-3* T-DNA.**

940 **Table S3. A hemizygous transgene *pEC-gRBR* partially restores fertility of *rbr-***  
941 **3 gametophytes in *rbr-3/RBR; pEC1-gRBR<sup>h</sup>* background.**

942 **Table S4. Progeny test confirms partial ‘two independent loci’**  
943 **complementation of *rbr-3* allele with *pEC-gRBR* in *rbr-3/RBR; pEC-gRBR<sup>h</sup>***  
944 **background. Note that offspring was scored based on antibiotic resistance of**  
945 ***rbr-3* T-DNA.**

946 **Table S5. Previously validated egg cell expressed transcripts showing**  
947 **deregulation in *rbr-3* ovule transcriptome**

948 **Table S6. List of RBR-regulated transcription factors, and stress and stimulus-**  
949 **responsive transcripts in the egg cell, subtracted from the ovule**  
950 **transcriptomes**

951 **Table S7. List of egg cell-expressed RBR interactors used for building protein**  
952 **interaction network.**

953 **Fig. S1. Overall gene ontology enrichment of stress and stimulus responsive**  
954 **genes and transcription factors in *rbr-3* egg cells. Gene ontology clustering for**

955 abiotic stress and stimulus enriched (A) or depleted (B) in *rbr-3* ovules, and enriched  
956 (C) or depleted (D) in *rbr-3* egg cells.

957 **Fig. S2. MYB64 and MYB119 transcripts in the mature embryo sac.** mRNA *in*  
958 *situ* hybridization: (A) Sense (S) probes shows no signal, while anti-sense probes  
959 (AS) detect (B) *MYB64* and (C) *MYB119* mRNA in the mature embryo sac, and  
960 specifically in the egg cell. Scale bar=20 $\mu$ m.

961 **Fig. S3. Chromatin immunoprecipitation in reproductive tissues in comparison**  
962 **to vegetative stages in *Arabidopsis*.** (A) ChIP for RBR or (B) for the PRC2-specific  
963 H3K27me3 binding. Relative real-time qPCR data normalized by input. *PCNA* locus  
964 was used as a positive control for RBR binding but negative for H3K27me3.

965 Significant difference is indicated between seedling and inflorescence tissues: \*\* $\alpha \leq$   
966 0.01; \* $\alpha \leq$  0.05.

967 **Fig. S4. RBR interacts with egg-cell expressed transcription factors.** (A) RBR  
968 protein-protein interactions identified by LexA-based yeast-two-hybrid assay. (B)  
969 Relative nuclei fluorescence intensity in BiFC assay with background subtraction. C-  
970 Ven-RBR was tested with the respective N-Ven-protein fusions.

971 **Fig. S5. Cell-cycle-dependent expression of MYB64.** *MYB64* transcript signals  
972 change with cell cycle progression in synchronized *Arabidopsis* cell culture in an  
973 opposite manner to *RBR* [46].

974 **Fig. S6. RBR connects transcriptional regulation and stress response shared**  
975 **by PRC2.** A protein interaction network connecting RBR, cell cycle, transcription  
976 factors and stress-responsive genes. Transcription factors enriched in *rbr-3* egg cell  
977 transcriptome connect to stress responsive



